GEOPHYSICS, VOL. 72, NO. 5 (SEPTEMBER-OCTOBER 2007); P. E193–E204, 18 FIGS., 2 TABLES.
10.1190/1.2762224

Cross-property relations between electrical conductivity and the seismic velocity of rocks

José M. Carcione[1], Bjørn Ursin[2], and Janniche I. Nordskag[2]

ABSTRACT

Cross-property relations are useful when some rock properties can be measured more easily than other properties. Relations between electrical conductivity and seismic velocity, stiffness moduli, and density can be obtained by expressing the porosity in terms of those properties. There are many possible ways to combine the constitutive equations to obtain a relation, each one representing a given type of rock. The relations depend on the assumptions to obtain the constitutive equations. In the electromagnetic case, the equations involve Archie's law and its modifications for a conducting frame, the Hashin-Shtrikman (HS) bounds, and the self-similar and complex refraction-index method (CRIM) models. In the elastic case, the stress-strain relations are mainly based on the time-average equation, the HS bounds, and the Gassmann equation. Also, expressions for dry rocks and for anisotropic media, using Backus averaging, are analyzed. The relations are applied to a shale saturated with brine (overburden) and to a sandstone saturated with oil (reservoir). Tests with sections of a North Sea well log show that the best fit is given by the relation between the Gassmann velocity and the CRIM, self-similar, and Archie models for the conductivity.

INTRODUCTION

Electrical, seismic, and electromagnetic methods can be used for noninvasive determination of subsurface physical and chemical properties. Seismic measurements provide wave velocities and attenuations, which can be translated to stiffness and quality factor, while electromagnetic data provide electromagnetic velocity and attenuation, which can be translated to dielectric constant and electrical conductivity. Most of the relevant properties for the oil-exploration problem are represented by electrical conductivity and wave velocity. Hence, it is important to obtain relationships between these physical quantities and the composition of the overburden and reservoir, including the saturating fluids.

The use of mixture theories is essential to obtain the conductivities and the velocities (e.g., Schön, 1996). We first establish the different constitutive equations. Mainly, the electromagnetic theories involve Archie's law (Archie, 1942) and its modifications for a conducting frame, the Hashin-Shtrikman (HS) bounds, and the self-similar and complex refraction-index method (CRIM) models. The main elastic models are the time-average equation, the HS bounds, and the Gassmann equation (e.g., Mavko et al., 1998). Also, expressions for dry rocks are considered, and Backus averaging to model anisotropic media is used to derive relations between tensor components. An example of the use of Backus averaging is given by Kennedy and Herrick (2004), who derive the porosity and saturation exponents of Archie's law, and obtain horizontal and vertical formation factors.

Thus, we develop new theories relating the electrical conductivity and the seismic velocity, i.e., knowing the conductivity, the P-wave velocity can be obtained, and vice versa. This is important in the sense that if one property, e.g., electrical conductivity, can be more easily measured than seismic velocity, the latter can be obtained by using a cross-property relation. The importance of such relations has been pointed out by Berryman and Milton (1988) and Gibiansky and Torquato (1995). Relations between various effective properties have been investigated in several works. In the classical paper of Bristow (1960), an explicit connection between the conductivity and the elastic moduli of a solid with cracks is derived. Other relevant articles are Berryman and Milton (1988), Gibiansky and Torquato (1995, 1996a, b), and Kachanov et al. (2001). Examples of relations to interpret logging data are given in Brito Dos Santos et al. (1988), who use a self-similar model for the conductivity and the time-average equation for the seismic velocity, and in Hacikoylu et al. (2006), who use the lower HS bound for the resistivity and Raymer's equation for the seismic velocity. The general approach to establish vari-

Manuscript received by the Editor November 15, 2006; revised manuscript received May 3, 2007; published online August 14, 2007.
[1]Istituto Nazionale di Oceanografia e di Geofisica Sperimentale (OGS), Trieste, Italy. E-mail: jcarcione@ogs.trieste.it.
[2]Norges Teknisk-Naturvitenskapelige Universitet (NTNU), Department of Petroleum Engineering and Applied Geophysics, Trondheim, Norway. E-mail: bjornu@ipt.ntnu.no; janniche.nordskag@ntnu.no.

ous cross-property relations is outlined by Milton (1997); see also the recent review of Markov (1999).

We consider the electrical conductivity/seismic velocity relations for the overburden (shale) and the reservoir (sandstone). Porosity is the property that allows us to establish the relations. One may use different mixtures theories to obtain the electromagnetic and seismic properties, and then combine these theories in different ways. For instance, Archie's law or the CRIM model combined with the time-average equation are two possible choices. Another choice is to relate the Gassmann equation with the different electromagnetic constitutive equations. Other possibilities involve the HS bounds and the self-similar equation. In the case of plane-layered composites, we consider Backus averaging to relate the conductivity and stiffness tensors, where the common property is the material proportion. The possibilities are multiple, and the subject is relatively new to draw definite conclusions; see, for instance, a controversial discussion by Ikwuakor (2007) on this topic. It is essential to perform laboratory experiments to provide controlled and reliable data.

The problem of electrical conductivity is mathematically equivalent to the ones of thermal conductivity, dielectric permittivity, and magnetic permeability; therefore, the approach can be applied to the mentioned physical properties as well.

THE BASIC APPROACH

The key property to relate the electrical conductivity to the P-wave velocity (or to the stiffness) is the porosity. Assume that the conductivity and velocity have the form

$$\sigma = f(\phi), \quad \text{and} \quad v = g(\phi), \tag{1}$$

where ϕ is the porosity. Then, the relation is given by

$$\sigma = f[g^{-1}(v)]. \tag{2}$$

This simple 1D concept is quite general and can be applied to higher spatial dimensions and the case of anisotropy (e.g., Kachanov et al., 2001).

CONSTITUTIVE EQUATIONS

We present in this section the constitutive equations relating the physical properties to the porosity.

Electromagnetism

Averages

The simplest (nonphysical) models for the electrical conductivity of a composite medium are the following averages:

$$\sigma = \sum_{i=1}^{N} p_i\sigma_i, \text{ arithmetic},$$
$$\sigma = \left(\sum_{i=1}^{N} \frac{p_i}{\sigma_i}\right)^{-1}, \text{ harmonic},$$
$$\sigma = \prod_{i=1}^{N} \sigma_i^{p_i}, \text{ geometric}, \tag{3}$$

where σ_i and p_i are the conductivity and volume fraction of phase i, respectively.

Archie's law and its modifications

The original form of Archie's law (Archie, 1942) is

$$\sigma = \sigma_f F^{-1} = \sigma_f \phi^m, \tag{4}$$

where σ_f is the conductivity of water, brine, or the fluid filling the pores; $F = \phi^{-m}$ is the formation factor; and m is the cementation or form factor.

Equation 4 has been designed for clean sands. In the presence of clay minerals, which are good conductors, the law has been modified. De Witte (1957) proposed

$$\sigma = G_1 + \sigma_f G_2. \tag{5}$$

A second model (Bussian, 1983) considers explicitly the conductivity of the clay particles σ_s:

$$\sigma = \left(\frac{1 - \sigma_s/\sigma_f}{1 - \sigma_s/\sigma}\right)^m \sigma_f \phi^m. \tag{6}$$

The model of Hermance (1979) is a particular case when $m = 1$ in the previous expression between parentheses,

$$\sigma = (\sigma_f - \sigma_s)\phi^m + \sigma_s = (1 - \phi^m)\sigma_s + \sigma_f\phi^m. \tag{7}$$

If $\sigma_s \to 0$, we obtain Archie's law. Equations 5 and 7 are identical for $G_1 = \sigma_s(1 - \phi^m)$ and $G_2 = F^{-1}$.

Finally, the model of Glover et al. (2000) has the form

$$\sigma = (1 - \phi)^p \sigma_s + \sigma_f \phi^m, \tag{8}$$

where each phase has its own connectivity and a representative exponent (m and p). Large exponents occur for low connectivity phases, and small exponents occur for high connectivity phases. The choice

$$p = \frac{\log(1 - \phi^m)}{\log(1 - \phi)} \tag{9}$$

gives Hermance's model. Glover et al. (2006) derive expressions for permeability as a function of electric conductivity.

HS models

HS bounds for the conductivity, for a system of N components, are

$$\sigma_{\mathrm{HS}}^- = \mathcal{S}(\sigma_{\min}) \le \sigma \le \mathcal{S}(\sigma_{\max}) = \sigma_{\mathrm{HS}}^+, \tag{10}$$

where

$$\mathcal{S}(x) = \left(\sum_{i=1}^{N} \frac{p_i}{\sigma_i + 2x}\right)^{-1} - 2x, \tag{11}$$

where p_i is the volume fraction of the phase i. The HS bounds, in the electromagnetic and elastic cases, are valid for isotropic media.

A two-component porous medium composed of grains, of conductivity σ_s, and water, of conductivity σ_f, such that $\sigma_{\min} = \sigma_s \le \sigma_f = \sigma_{\max}$, has the following bounds:

$$\sigma_{\mathrm{HS}}^{-} = \left(\frac{1-\phi}{3\sigma_s} + \frac{\phi}{\sigma_f + 2\sigma_s}\right)^{-1} - 2\sigma_s,$$
$$\sigma_{\mathrm{HS}}^{+} = \left(\frac{1-\phi}{\sigma_s + 2\sigma_f} + \frac{\phi}{3\sigma_f}\right)^{-1} - 2\sigma_f. \tag{12}$$

When the case is $\sigma_{\min} = \sigma_f \leq \sigma_s = \sigma_{\max}$, the bounds should be reversed, i.e., the lower bound becomes the upper bound, and vice versa (Berryman, 1995).

The so-called Clausius-Mossoti formula for a two-component medium consisting of water containing spherical grains is the HS upper bound (e.g., Berryman, 1995).

The inverse of the formation factor is $F^{-1} = \sigma/\sigma_f$, such that for insulating particles embedded in a conducting fluid, $F^{-1} = 1$ for the fluid and $F^{-1} = 0$ for the particles. The lower bound of F is the upper bound of F^{-1}. Then, using equation 10 for F^{-1}, and because $F_{\max}^{-1} = 1$, we obtain $F_{\mathrm{HS}}^{-1} = 2\phi/(3-\phi)$, which yields the following equation:

$$F_{\mathrm{HS}}^{-} = \frac{3-\phi}{2\phi} = \frac{\sigma_f}{\sigma_{\mathrm{HS}}^{+}}. \tag{13}$$

The formation factor corresponding to insulating particles embedded in a conducting fluid must be greater than the HS lower bound (e.g., Berryman, 1995).

CRIM and Lichtnecker-Rother models

The CRIM for negligible permittivity can be expressed as

$$\sigma = \left[\sum_{i=1}^{N} p_i(\sigma_i)^{1/\gamma}\right]^{\gamma}, \quad \gamma = 2 \tag{14}$$

(Schön, 1996). (Note that the complex permittivity is $\epsilon + i\sigma/\omega$, where ϵ is the permittivity. In this case $\epsilon = 0$).) If γ is a free parameter, the equation is termed Lichtnecker-Rother formula. This model is very simple and of easy implementation. It uses the ray approximation. (The traveltime in phase i is inversely proportional to the electromagnetic velocity, which in turn is inversely proportional to the square root of the complex dielectric constant.)

Self-similar model

In the self-similar model (Sen et al., 1981; Carcione et al., 2003), the conductivity of the composite satisfies

$$0 = \sum_{i=1}^{N} p_i\left(\frac{\sigma - \sigma_i}{2\sigma + \sigma_i}\right). \tag{15}$$

For two constituents (solid and fluid), the solution is given by

$$\phi = f(\sigma, \sigma_s, \sigma_f) = \left(\frac{\sigma_s - \sigma}{\sigma_s - \sigma_f}\right)\left(\frac{\sigma_f}{\sigma}\right)^{W}, \tag{16}$$

where $W = 1/3$ for spherical inclusions. In this case, we may rewrite equation 16 as

$$(1-\hat{\sigma})^3 = a\hat{\sigma}, \tag{17}$$

where

$$\hat{\sigma} = \frac{\sigma}{\sigma_s}, \quad a = \frac{\sigma_s}{\sigma_f}\left(1 - \frac{\sigma_f}{\sigma_s}\right)^3 \phi^3 \tag{18}$$

(Carcione and Seriani, 2000). This equation has the following solutions

$$\hat{\sigma}_1 = 1 - \left(\frac{a}{3}\right)^{1/3}\left[\left(\frac{2a}{\gamma}\right)^{1/3} - \left(\frac{\gamma}{6}\right)^{1/3}\right],$$
$$\hat{\sigma}_2 = 1 + \left(\frac{a}{12}\right)^{1/3}\left[z_0\left(\frac{a}{\gamma}\right)^{1/3} - z_0^*\left(\frac{\gamma}{12}\right)^{1/3}\right],$$
$$\hat{\sigma}_3 = 1 + \left(\frac{a}{12}\right)^{1/3}\left[z_0^*\left(\frac{a}{\gamma}\right)^{1/3} - z_0\left(\frac{\gamma}{12}\right)^{1/3}\right], \tag{19}$$

where

$$\gamma = \sqrt{3(27+4a)} - 9, \quad z_0 = 1 + \sqrt{-3}. \tag{20}$$

The physical solution is that approaching σ_f in the limit $\phi \to 1$.

When $W \neq 1/3$, we have the Hanai-Bruggeman relationship (Schön, 1996), which describes a porous medium of arbitrary grain shape.

For insulating particles embedded in a conducting fluid, we obtain

$$\sigma = \sigma_f \phi^{1/(1-W)}, \quad F = \phi^{1/(W-1)}, \quad m = 1/(1-W). \tag{21}$$

Bussian's equation 6 is identical to equation 16. Note that $m = 3/2$ for spherical particles.

Backus averaging

The electromagnetic properties of finely plane-layered media can be obtained by using Backus averaging (e.g., Carcione, 2007). Let us consider a plane-layered medium, where each layer is homogeneous, isotropic, and thin compared to the wavelength of the electromagnetic wave. If the layer interfaces are parallel to the (x,y)-plane, the properties are independent of x and y, and may vary with z. The equivalent medium is transversely isotropic and can be described with two components of the conductivity tensor:

$$\begin{pmatrix}\sigma_{11}\\ \sigma_{33}^{-1}\end{pmatrix} = \begin{pmatrix}\sigma_1 & \sigma_2\\ \sigma_1^{-1} & \sigma_2^{-1}\end{pmatrix}\begin{pmatrix}p_1\\ p_2\end{pmatrix}, \tag{22}$$

where we have assumed that there are two thin layers of proportion p_1 and p_2 and conductivity σ_1 and σ_2. The proportions can be expressed as

$$p_1 = \frac{\sigma_{11} - \sigma_2}{\sigma_1 - \sigma_2} = \frac{\sigma_{33}^{-1} - \sigma_2^{-1}}{\sigma_1^{-1} - \sigma_2^{-1}}, \quad \text{and} \quad p_2 = 1 - p_2. \tag{23}$$

Elasticity

Averages

As in the electromagnetic case, we can obtain the P-wave velocity of a composite medium with the following averages:

$$v_P = \sum_{i=1}^{N} p_i v_i, \text{ arithmetic},$$

$$v_P = \left(\sum_{i=1}^{N} \frac{p_i}{v_i} \right)^{-1}, \text{ harmonic},$$

$$v_P = \prod_{i=1}^{N} v_i^{p_i}, \text{ geometric}, \tag{24}$$

where v_i and p_i are the P-wave velocity and volume fraction of phase i, respectively.

Time-average equation

This equation is the harmonic average given in the previous section. The P-wave velocity of a fully saturated porous medium is

$$v_P = \left(\frac{\phi}{v_f} + \frac{1-\phi}{v_s} \right)^{-1}, \tag{25}$$

where v_f is the wave velocity of the fluid, and v_s is the P-wave velocity of the grains.

Raymer's equation

This equation (Raymer et al., 1980) is used for consolidated sands. It is given by

$$v_P = (1-\phi)^2 v_s + \phi v_f. \tag{26}$$

HS models

The HS lower bound of the bulk modulus corresponding to a two-component porous medium composed of grains, of bulk and shear moduli K_s and μ_s, and water, of bulk modulus K_f, is

$$K_{\mathrm{HS}}^- = \left(\frac{\phi}{K_f} + \frac{1-\phi}{K_s} \right)^{-1}, \tag{27}$$

which is the Reuss average (e.g., Berryman, 1995). The upper bound is given by

$$K_{\mathrm{HS}}^+ = \left(\frac{1-\phi}{K_s + x} + \frac{\phi}{K_f + x} \right)^{-1} - x, \quad x = \frac{4}{3}\mu_s. \tag{28}$$

The corresponding bounds for the shear modulus are

$$\mu_{\mathrm{HS}}^- = 0, \quad \mu_{\mathrm{HS}}^+ = \left(\frac{1-\phi}{\mu_s + x} + \frac{\phi}{x} \right)^{-1} - x,$$

$$x = \frac{\mu_s}{6}\left(\frac{9K_s + 8\mu_s}{K_s + 2\mu_s} \right). \tag{29}$$

The velocities are given by

$$v_P^- = \sqrt{\frac{K_{\mathrm{HS}}^-}{\rho}}, \quad \text{and} \quad v_P^+ = \sqrt{\frac{1}{\rho}\left(K_{\mathrm{HS}}^+ + \frac{4}{3}\mu_{\mathrm{HS}}^+ \right)}. \tag{30}$$

Gassmann velocity

The P-wave velocity of a fully saturated porous medium is

$$v_G = \sqrt{\frac{1}{\rho}\left(K_G + \frac{4}{3}\mu_m \right)}, \tag{31}$$

where

$$K_G = \frac{K_s - K_m + \phi K_m (K_s/K_f - 1)}{1 - \phi - K_m/K_s + \phi K_s/K_f} \tag{32}$$

(e.g., Carcione, 2007) is a saturation (or undrained) bulk modulus, where K_m and μ_m are the bulk and shear moduli of the matrix, and K_s and K_f are the grain and fluid bulk moduli, respectively; the composite density is given by

$$\rho = (1-\phi)\rho_s + \phi\rho_f, \tag{33}$$

where ρ_s and ρ_f are the densities of the grain and fluid, respectively.

Backus averaging

In the case of a periodically layered medium, the equivalent medium is transversely isotropic, and one of the shear waves decouples from the other two wave modes. Usually, this pure mode is termed SH in the exploration-geophysics literature. For two constituents, the effective elastic constants involved in the description of this wave are given by

$$\begin{pmatrix} c_{66} \\ c_{44}^{-1} \end{pmatrix} = \begin{pmatrix} \mu_1 & \mu_2 \\ \mu_1^{-1} & \mu_2^{-1} \end{pmatrix} \begin{pmatrix} p_1 \\ p_2 \end{pmatrix}, \tag{34}$$

where μ_1 and μ_2 are the shear moduli of the single constituents. The other elastic constants, such as c_{11}, c_{33}, and c_{13} for a periodically layered medium of two isotropic thin layers, are given by Postma (1955).

The proportions can be expressed as

$$p_1 = \frac{c_{66} - \mu_2}{\mu_1 - \mu_2} = \frac{c_{44}^{-1} - \mu_2^{-1}}{\mu_1^{-1} - \mu_2^{-1}}, \quad \text{and} \quad p_2 = 1 - p_1. \tag{35}$$

CROSS-PROPERTY RELATIONS

There are many possibilities to establish cross-property relations. Several of them are presented in the following section. Each relation may represent a given type of rock, depending on the assumptions to obtain the involved constitutive equations. In practice, comparison to experimental data is necessary.

Dry rocks

Expressions for dry rocks are given in the following, where dry means $\sigma_f = 0$ and $K_f = 0$.

Bristow

Bristow (1960) obtained relations between the dry-rock bulk modulus K_m and dry-rock conductivity σ_m for randomly oriented, penny-shaped cracks of zero conductivity embedded in an isotropic medium:

$$\frac{K_s - K_m}{K_m} = \frac{2(1-\nu_s^2)}{1-2\nu_s}\frac{\sigma_s - \sigma_m}{\sigma_m}, \tag{36}$$

where K_s and ν_s are the bulk modulus and Poisson ratio, respectively, of the solid medium. The equivalent relation for the dry-rock shear modulus μ_m is

$$\frac{\mu_s - \mu_m}{\mu_m} = \frac{4}{5}(1-\nu_s)(5-\nu_s)\left(\frac{\sigma_s - \sigma_m}{\sigma_m}\right), \tag{37}$$

where μ_s is the shear modulus of the solid medium (e.g., Sevostianov and Kachanov, 2007).

Berryman-Milton bounds

In this case, $\sigma_f \neq 0$, but $K_f = 0$. Berryman and Milton (1988) derived the following bounds for the electrical conductivity σ and bulk modulus K of a porous insulator saturated with a conducting fluid:

$$\frac{1}{2}\frac{(1-\phi)\sigma}{(\phi\sigma_f - \sigma)} \leq 1 - \frac{3\phi K}{4\mu_s(1-\phi-K/K_s)}, \tag{38}$$

where $\sigma_s = 0$.

The corresponding bound for the shear modulus is

$$\frac{1}{2}\frac{(1-\phi)\sigma}{(\phi\sigma_f - \sigma)} \leq \frac{21}{5-21B}\left(1 + B - \frac{6A\phi\mu}{(1-\phi)\mu_s - \mu}\right), \tag{39}$$

where

$$A = \frac{6(K_s + 2\mu_s)^2}{(3K_s + \mu_s)^2}, \quad B = \frac{5\mu_s(4K_s + 3\mu_s)}{(3K_s + \mu_s)^2} \tag{40}$$

(Sevostianov and Kachanov, 2007).

Gibiansky-Torquato bound

Gibiansky and Torquato (1996b) derived the following relation for (cracked) dry rocks:

$$\frac{1}{K_m} - \frac{1}{K_s} \geq \frac{3\sigma_s}{2\mu_s}\frac{1-\nu_s}{1+\nu_s}\left(\frac{1}{\sigma_m} - \frac{1}{\sigma_s}\right) \tag{41}$$

(e.g., Sevostianov and Kachanov, 2007).

Wet rocks

Milton bounds

Milton (1981) derived the following inequalities for the composite bulk and shear moduli, K and μ, respectively:

$$\frac{K}{K_s} \leq \frac{\sigma}{\sigma_s}, \quad \frac{\mu}{K_s} \leq \frac{3\sigma}{2\sigma_s}, \tag{42}$$

where $K_f/K_s \leq \sigma_f/\sigma_s$ (e.g., Sevostianov and Kachanov, 2007). In particular, for dry rocks, $K_f = 0$, $\sigma_f = 0$, and the bounds are equally valid.

Archie/time-average

One of the simplest relations is the combination of Archie's law 4 and the time-average equation 25. Then, equation 2 reads

$$\sigma = \sigma_f\left(\frac{v_s/v_P - 1}{v_s/v_f - 1}\right)^m, \tag{43}$$

where σ_f is the conductivity of the fluid.

Archie/Raymer

Combining Raymer's equation 26 and Archie's law gives

$$v_P = \left[1 - \left(\frac{\sigma}{\sigma_f}\right)^{1/m}\right]^2 v_s + \left(\frac{\sigma}{\sigma_f}\right)^{1/m} v_f. \tag{44}$$

Glover et al./time-average

The time-average equation 25 and Glover et al. (2000, equation 8) give

$$\sigma = (1-\phi)^p\sigma_s + \sigma_f\phi^m, \quad \phi = \frac{1/v_P - 1/v_s}{1/v_f - 1/v_s}. \tag{45}$$

Hermance/time-average

The time-average equation 25 and Hermance's equation 7 give

$$\sigma = (\sigma_f - \sigma_s)\phi^m + \sigma_s, \quad \phi = \frac{1/v_P - 1/v_s}{1/v_f - 1/v_s}. \tag{46}$$

Self-similar/time-average

For a conducting matrix, Brito Dos Santos et al. (1988) obtained the following relation from the self-similar and time-average equations 16 and 25:

$$v_P = \left[\left(\frac{1}{v_f} - \frac{1}{v_s}\right)\left(\frac{\sigma_s - \sigma}{\sigma_s - \sigma_f}\right)\left(\frac{\sigma_f}{\sigma}\right)^{1-1/m} + \frac{1}{v_s}\right]^{-1}. \tag{47}$$

HS/Raymer

The relation used by Hacikoylu et al. (2006), based on Raymer's equation 26 and the HS lower bound 13, is

$$v_P = (1-\phi+\phi_p)^2 v_s + (\phi - \phi_p)v_f, \quad \phi = \frac{3\sigma}{\sigma + 2\sigma_f}, \tag{48}$$

where ϕ_p is a percolation porosity ($\phi_p = 0.4$ in Hacikoylu et al. (2006)). We assume $\phi_p = 0$ in our calculations.

Faust

Faust's empirical relation is

$$v_P[\text{km/s}] = 2.2888\left(z[\text{km}]\frac{\sigma}{\sigma_f}\right)^{1/6}, \tag{49}$$

where z is the depth (Faust, 1953).

HS models

We now combine the HS electromagnetic and seismic models. Let us consider a two-phase medium composed of a solid matrix and a fluid. Equation 12 gives

$$\phi = \left(\frac{\sigma_s - \sigma_{\mathrm{HS}}^-}{\sigma_s - \sigma_f}\right)\left(\frac{\sigma_f + 2\sigma_s}{\sigma_{\mathrm{HS}}^- + 2\sigma_s}\right) = \left(\frac{\sigma_s - \sigma_{\mathrm{HS}}^+}{\sigma_s - \sigma_f}\right)\left(\frac{3\sigma_f}{\sigma_{\mathrm{HS}}^+ + 2\sigma_f}\right). \quad (50)$$

The cross-property relation given by the lower HS bounds combine this equation and equation 27:

$$K_{\mathrm{HS}}^- = \left[\left(\frac{\sigma_s - \sigma_{\mathrm{HS}}^-}{\sigma_s - \sigma_f}\right)\left(\frac{\sigma_f + 2\sigma_s}{\sigma_{\mathrm{HS}}^- + 2\sigma_s}\right)\left(\frac{1}{K_f} - \frac{1}{K_s}\right) + \frac{1}{K_s}\right]^{-1}. \quad (51)$$

If $\sigma_f \leq \sigma_s$, σ_{HS}^- must be replaced by σ_{HS}^+. The wave velocity is given by equation 30, and the density is given by equation 33:

$$\rho(\sigma) = (\rho_f - \rho_s)\phi(\sigma) + \rho_s. \quad (52)$$

The cross-property relations corresponding to the upper HS bounds involve equations 50, 28, and 29, and the wave velocity is given by equation 30.

Gassmann-based relations

To use the Gassmann equation, we assume a model for the dry-rock moduli as a function of porosity, i.e., $K_m(\phi)$ and $\mu_m(\phi)$. Then, we replace $\phi = \phi(\sigma)$ into the Gassmann equation. According to equation 32, the relation between the bulk modulus and the conductivity is

$$K = K_G = \frac{K_s - K_m(\phi) + \phi K_m(\phi)(K_s/K_f - 1)}{1 - \phi - K_m(\phi)/K_s + \phi K_s/K_f}, \quad (53)$$

where

$$\phi = \left(\frac{\sigma}{\sigma_f}\right)^{1/m}, \quad \text{Archie},$$

$$\phi = \left(\frac{\sigma - \sigma_s}{\sigma_f - \sigma_s}\right)^{1/m}, \quad \text{Hermance},$$

$$\phi = \left(\frac{\sigma^{1/\gamma} - \sigma_s^{1/\gamma}}{\sigma_f^{1/\gamma} - \sigma_s^{1/\gamma}}\right), \quad \gamma = 2, \text{ CRIM},$$

$$\phi = \left(\frac{\sigma - \sigma_s}{\sigma_f - \sigma_s}\right)\left(\frac{\sigma_f}{\sigma}\right)^{1-1/m}, \quad \text{self-similar},$$

$$\phi = \left(\frac{\sigma_s - \sigma}{\sigma_s - \sigma_f}\right)\left(\frac{\sigma_f + 2\sigma_s}{\sigma + 2\sigma_s}\right), \quad \text{HS lower bound},$$

$$\phi = \left(\frac{\sigma_s - \sigma}{\sigma_s - \sigma_f}\right)\left(\frac{3\sigma_f}{\sigma + 2\sigma_f}\right), \quad \text{HS upper bound}, \quad (54)$$

corresponding to equations 4, 7, 14, 16, and 50, respectively. The HS bounds are reversed if $\sigma_f \leq \sigma_s$.

We consider the model of Krief et al. (1990), to obtain the dry-rock moduli K_m and μ_m as a function of porosity. The porosity dependence of the rock frame should be consistent with the concept of critical porosity, because the moduli should be small above a certain value of the porosity (usually from 0.4 to 0.6). This dependence is determined by the empirical coefficient A (see equation 55). The bulk and shear moduli of the rock frame are

$$K_m = K_s(1 - \phi)^{(1-\phi+A)/(1-\phi)},$$

$$\mu_m = \left(\frac{\mu_s}{K_s}\right)K_m. \quad (55)$$

Krief et al. (1990) set the A parameter to 3 regardless of the lithology. Alternatively, the value of A can be estimated by using data from the study area. We assume $A = 3$ in our calculations.

An alternative method to compute the dry-rock moduli including the effects of pore and confining pressures is the Hertz-Mindlin model (Mindlin, 1949; Carcione et al., 2006a, b). On the other hand, the pressure effects can be incorporated in the electromagnetic constitutive equations considering, for instance, that for sandstones it is $\phi = \phi(p_c - p)$, where p_c and p are the confining (overburden) and pore-fluid pressures (e.g., Carcione, 2007).

Layered media: Backus-based relations

In this case, instead of the porosity, we eliminate the material proportions p_1 and p_2 from equations 22 and 34 to obtain relations between the conductivity components and the elasticity components. The relations are

$$\frac{\sigma_{11} - \sigma_2}{\sigma_1 - \sigma_2} = \frac{c_{66} - \mu_2}{\mu_1 - \mu_2} \quad (56)$$

and

$$\frac{\sigma_{33}^{-1} - \sigma_2^{-1}}{\sigma_1^{-1} - \sigma_2^{-1}} = \frac{c_{44}^{-1} - \mu_2^{-1}}{\mu_1^{-1} - \mu_2^{-1}}. \quad (57)$$

Other similar relations can be obtained, in principle, between the conductivity components and the elasticity constants c_{11}, c_{33}, c_{12}, and c_{13}. (Note that $c_{66} = (c_{11} - c_{12})/2$.) The utility of these relations is still uncertain; although the proportions are not present in the equations, they depend on the properties of the single constituents, which, in practice, are not easy to measure.

RESULTS AND DISCUSSION

We consider a fully saturated shale (overburden) and a sandstone saturated with light oil (reservoir). The properties of the single constituents are shown in Table 1. In the first case, the fluid has a higher conductivity than the frame, while oil has a lower conductivity than the sandstone grains. The moduli of the material composing the frames are typical for composite clay and quartz, respectively.

Table 1. Material properties.

Rock	σ_s (S/m)	σ_f (S/m)	K_s (GPa)	μ_s (GPa)	ρ_s (g/cm^3)	K_f (GPa)	ρ_f (g/cm^3)
Overburden (shale-brine)	0.1[3]	0.4[4]	20	15	2.5	2.25	1
Reservoir (sandstone-oil)	10^{-3}[5]	10^{-5}	39	40	2.65	0.57	0.7

[3] wet clay;
[4] 0.01 ppt of NaCl;
[5] wet quartz.

The electrical conductivity of the shale and sandstone as a function of porosity are given in Figures 1 and 2, respectively. The curves have opposite behavior. Increasing porosity (i.e., increasing fluid saturation) makes the shale more conductive and the sandstone more resistive. At zero porosity, the conductivity is that of the solid material. The geometric average, and the CRIM and self-similar models lie within the HS bounds, with the average almost coinciding with the lower HS bound in the case of the sandstone. The Glover and Hermance models are outside the bounds for the exponential values of the parameters $m = 2$ and $p = 0.15$. The value of m is a mean value commonly used for Archie's law, and the value of p is reported by Glover et al. (2000).

Figures 3 and 4 show the P-wave velocity versus porosity. At zero porosity, the velocity is that of the solid material. In this case, the ve-

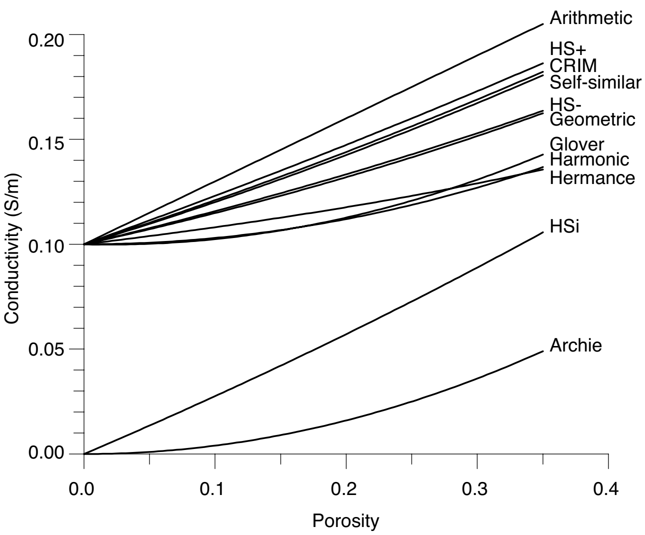

Figure 1. Conductivity as a function of porosity corresponding to different models of the overburden (shale saturated with brine). HSi and Archie assume a matrix with zero conductivity. HSi is an upper bound in this case. The Archie, Hermance, and Glover models assume $m = 2$ and $p = 0.15$. The last two models lie outside the HS bounds.

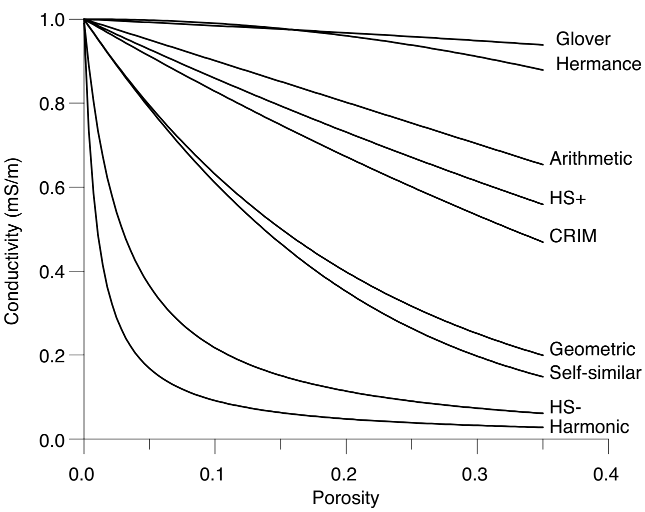

Figure 2. Conductivity as a function of porosity corresponding to different models of the reservoir (sandstone saturated with oil). The Archie, Hermance, and Glover models assume $m = 2$ and $p = 0.15$. Note that the last two models lie outside the HS bounds.

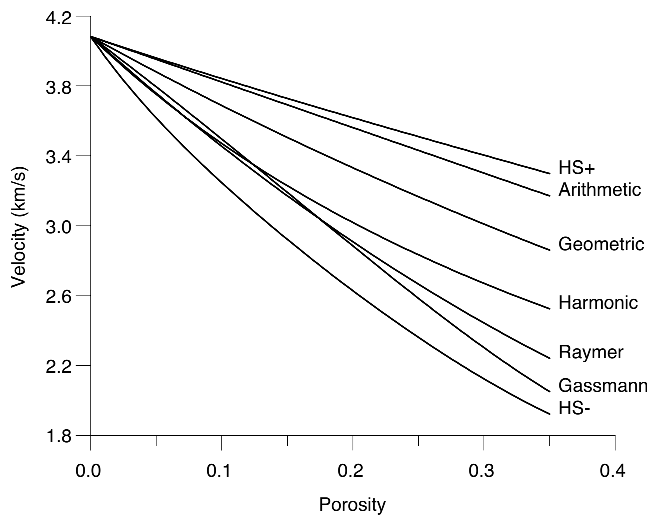

Figure 3. P-wave velocity as a function of porosity corresponding to different models of the overburden (shale saturated with brine). The harmonic average is the time-average equation.

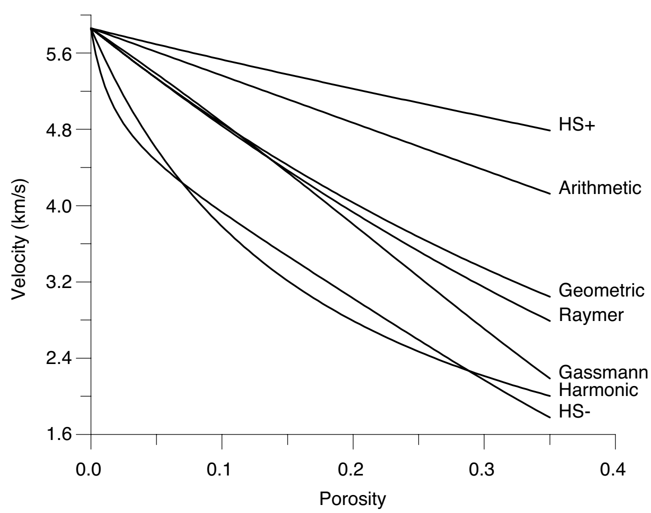

Figure 4. P-wave velocity as a function of porosity corresponding to different models of the reservoir (sandstone saturated with oil). The harmonic average is the time-average equation.

locity is decreasing for increasing porosity, since the fluids (brine and oil) have a smaller bulk modulus than that of the grains. All of the curves lie within the HS bounds, unless the time-average equation in a wide range of porosities of the sandstone.

We display in Figure 5 the cross-property relations for dry rocks. In this case, we assume a sandstone with K_s = 39 GPa and a grain conductivity of $\sigma_s = 0.1$ S/m. Note that when the bulk modulus is 39 GPa, the conductivity is that of the grain. The Milton and Gibiansky-Torquato curves are an upper bound for the dry-rock modulus. All of the other models lie above these bounds.

Figures 6 and 7 represent the relations for wet rocks, overburden, and reservoir, respectively. Faust's curve for $z = 2$ km is shown in the case of the sandstone. The Archie models assume $\sigma_s = 0$, while the other curves tend to the grain conductivity at the highest velocity, where $\phi = 0$. The curve corresponding to the Glover model exceeds the brine conductivity (0.4 S/m) for a narrow range of velocities. This is an artifact of this model. The models with nonzero grain conductivity give a similar behavior for the shale, but the self-similar/time-average curve is different from those based on the Glover and Hermance models, which are flat in a wide range of velocities. The self-similar/time-average curve should be more reliable because the self-similar curve lies within the HS bounds, as can be observed in Figure 2.

Combinations of the different electromagnetic constitutive equations with the Gassmann equation are shown in Figures 8 and 9, for the shale and the sandstone, respectively. At the low-velocity limit, the curves approach the conductivity of the fluid, which is much smaller than the grain conductivity of the sandstone. At the high-ve-

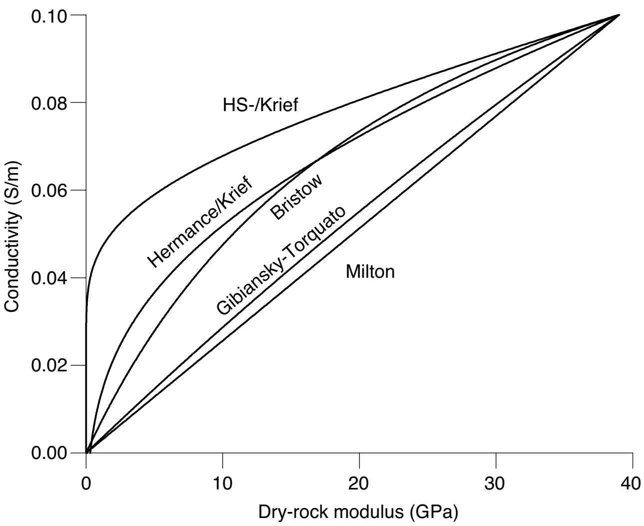

Figure 5. Cross-property relations for dry rocks. The Krief model (see equation 55) is combined with the Hermance model (equation 7) and with the lower HS bound (equation 12), where $\sigma_f = 0$ has been assumed. The expressions of the porosity for these models are $\phi = (1 - \sigma/\sigma_s)^{1/m}$ and $\phi = 2(\sigma_s - \sigma)/(\sigma + 2\sigma_s)$, respectively.

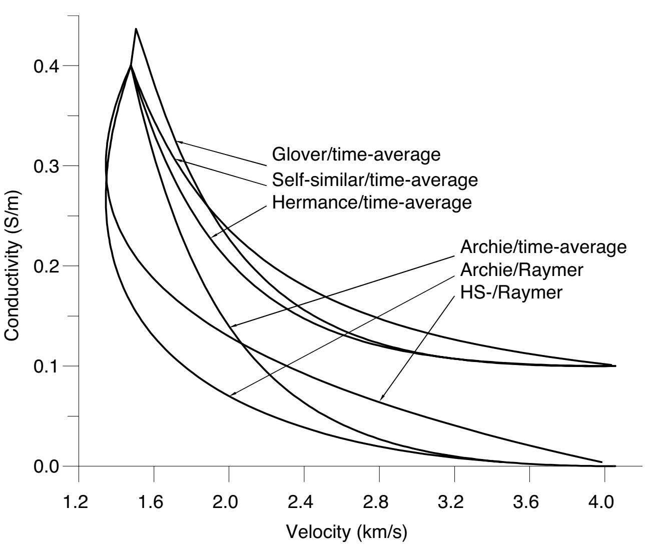

Figure 6. Cross-property relations for different models of the overburden (shale saturated with brine).

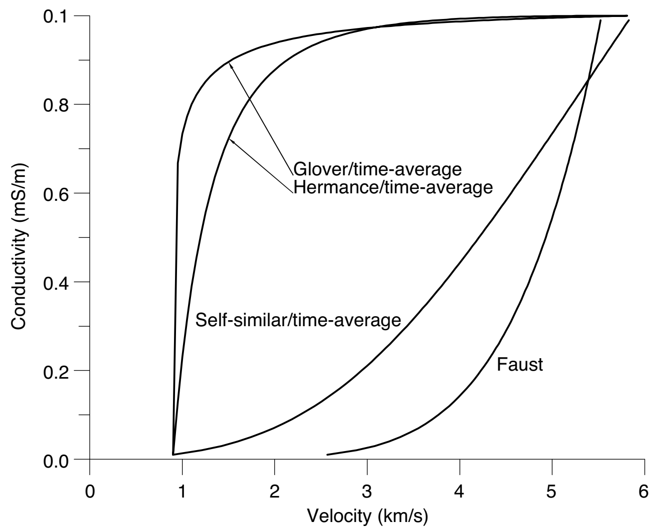

Figure 7. Cross-property relations for different models of the reservoir (sandstone saturated with oil). Archie-based relations are not shown because the conductivity is negligible (it is assumed that σ_s = 0). The Faust curve corresponds to 2-km depth.

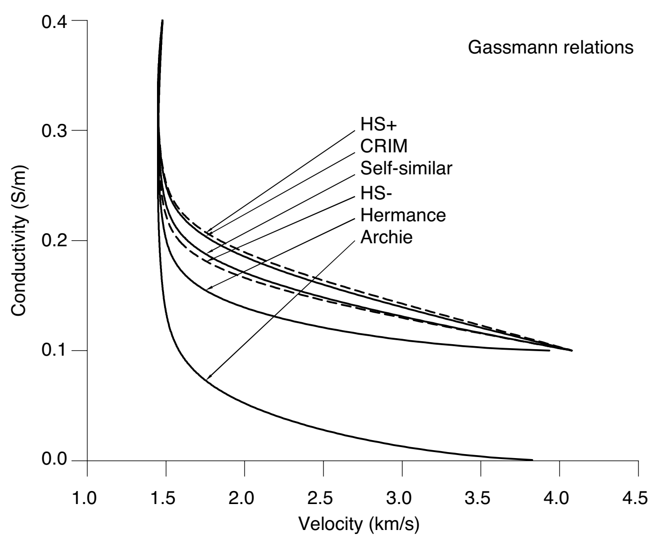

Figure 8. Cross-property relations for different conductivity models of the overburden (shale saturated with brine), combined with the Gassmann equation. The dashed lines correspond to the HS bounds.

locity limit, the conductivity is that of the grains (zero for Archie's model). It can be shown that the curves of Figure 8, corresponding to the bulk modulus, are within the Milton bound 42. The CRIM and self-similar curves lie within the HS bounds in both cases. These bounds are very tight for the shale. The trend in Figures 6–9 is that as the velocity of the shale increases, the conductivity decreases. The opposite behavior is verified for the sandstone.

Cross-property relations based only on HS bounds are shown in Figure 10. The curves based on the lower bound correspond to a suspension of grains in the fluid because the shear moduli are zero for all porosities. Then, the higher velocity limit is that of a suspension.

Finally, Figure 11 shows the relations between conductivity and velocity for an anisotropic medium, where v_{44} and v_{66} are the velocities of an SH wave propagating along the axis of symmetry and layering plane of an equivalent transversely isotropic medium, representing a periodic plane-layered system composed of two isotropic thin layers. In case (b), the conductivities of the single layers have been reversed with respect to case (a). As can be seen, the conductivity along the layering direction is always greater than along the direction of the symmetry axis.

More realistic relations can be obtained by using more complex theories. In particular, in the case of a reservoir rock, represented by a porous medium, the conductivity in the geoelectric frequency range can be obtained by using Pride's model (Pride, 1994; Carcione et al., 2003). (This model considers salinity and permeability.). On the other hand, the White et al. mesoscopic model can be used to calculate the seismic properties of a heterogeneous porous medium (White et al., 1975) (see also Carcione et al., 2003). Extension to the anisotropic case involves the Brown-Korringa relations, which are a generalization of the Gassmann equations (e.g., Carcione, 2007), and the work of Kachanov et al. (2001).

Comparison to real data

The data correspond to a well log at the Gullfaks field in the North Sea. The well is vertical and consists of sand and shale filled with brine. Figure 12 shows the velocity as a function of porosity, where two main well-distinguished sets of data points can be appreciated, representing a sandstone (high velocities) and a shale (low velocities). Using the physical properties given in Table 2, different velocity/porosity relations are represented in Figures 13 and 14, corresponding to shale and sandstone, respectively. The plots show that the data follow Gassmann's velocity. On the other hand, Figures 15 and 16 show the conductivity as a function of porosity for the shale and the sandstone, respectively, where we assume $W = 1/2$, i.e., $m = 2$. The shale data are in good agreement with the self-similar, CRIM, Glover and Hermance models. The curves of the last two models practically coincide. The sandstone data are better represented by the CRIM, self-similar, Archie, Glover and Hermance models, where the last four have the same curve in practice.

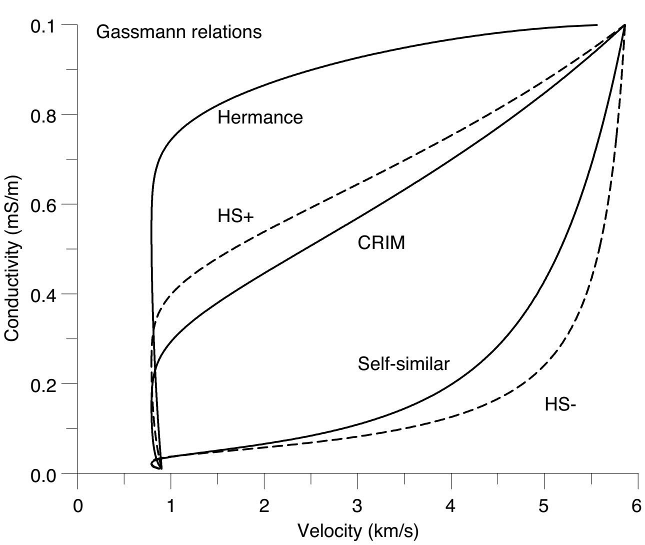

Figure 9. Cross-property relations for different conductivity models of the reservoir (sandstone saturated with oil), combined with the Gassmann equation. The dashed lines correspond to the HS bounds.

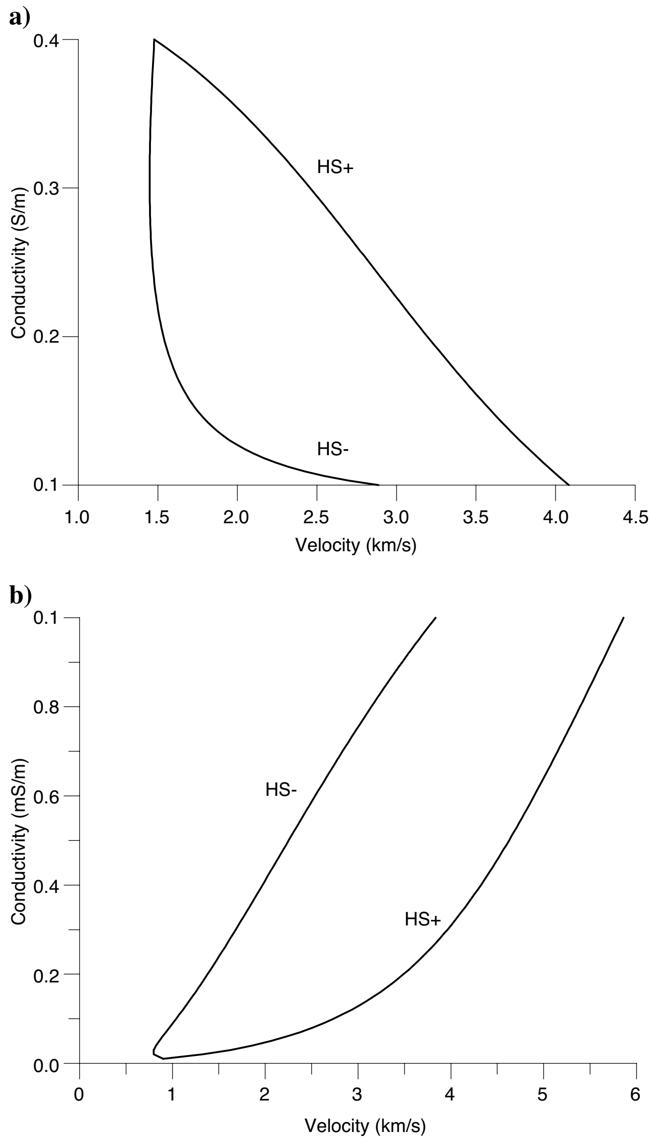

Figure 10. Cross-property relations for the electromagnetic and elastic HS models of the overburden (shale saturated with brine) (a) and reservoir (sandstone saturated with oil) (b).

Using the Gassmann model for the velocity and different models for the conductivity, we represent the relation between these quantities in Figures 17 and 18, for the shale and the sandstone, respectively. The shale data are within the HS bounds, and the Gassmann velocity model combined with the CRIM or with the self-similar electrical models gives the best fit to the data. The Faust model is also represented in Figure 17, but does not match the data and is outside the HS bounds. The sandstone data follow the HS bounds and, also in this case, the best fit is given by the combination Gassmann (velocity)/CRIM or self-similar or Archie (conductivity).

Hacikoylu et al. (2006) suggest a modified version of the Faust equation. However, there are several physical models that provide a reasonable fit of the data. Hence, we believe that there is no reason to use a purely empirical equation such as Faust's equation. Ikwuakor(2007) suggests the use of a time-average (harmonic) equation for the transit time combined with Archie's equation for the conductivity. Regarding our data, the time-average equation for the velocity does not constitute a good model to fit the data.

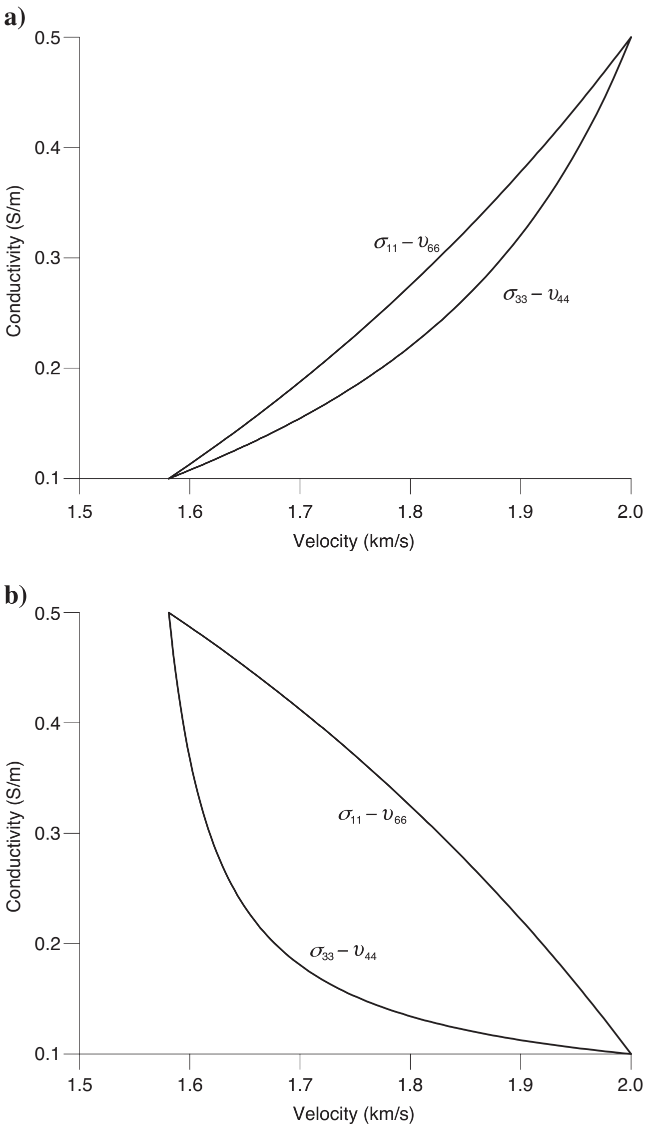

Figure 11. Cross-property relations corresponding to Backus averaging, where $v_{44} = \sqrt{c_{44}/\rho}$ and $v_{66} = \sqrt{c_{66}/\rho}$, and $\rho = p_1\rho_1 + p_2\rho_2$. Case (a) corresponds to $\sigma_1 = 0.1$ S/m, $\sigma_2 = 0.5$ S/m, $\mu_1 = 5$ GPa and $\mu_2 = 10$ GPa. In case (b), the conductivity components are $\sigma_1 = 0.5$ S/m and $\sigma_2 = 0.1$ S/m. The densities are $\rho_1 = 2$ g/cm^3 and $\rho_2 = 2.5$ g/cm^3.

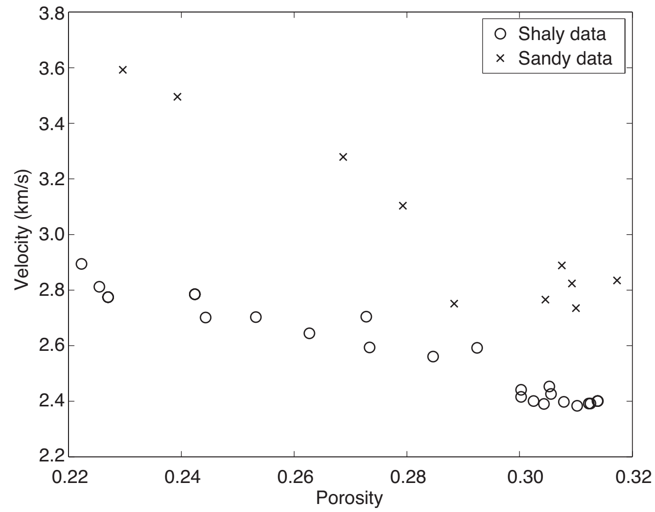

Figure 12. P-wave velocity as a function of porosity for a North Sea vertical well.

Table 2. Material properties at a North Sea well.

Medium	K (GPa)	μ (GPa)	ρ (g/cm^3)	σ (S/m)
Shale grains	25	20	2.65	0.2
Sand grains	39	40	2.65	0.01
Brine	2.25	0	1.03	15

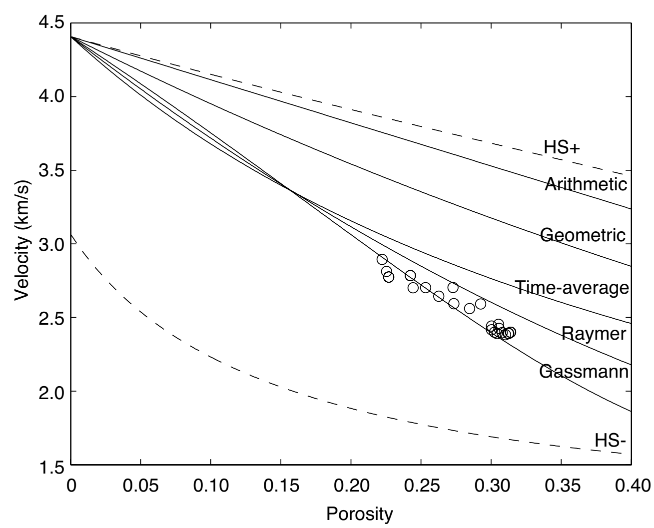

Figure 13. Different models of the P-wave velocity as a function of porosity and real data (circles), corresponding to the shaly section of the well.

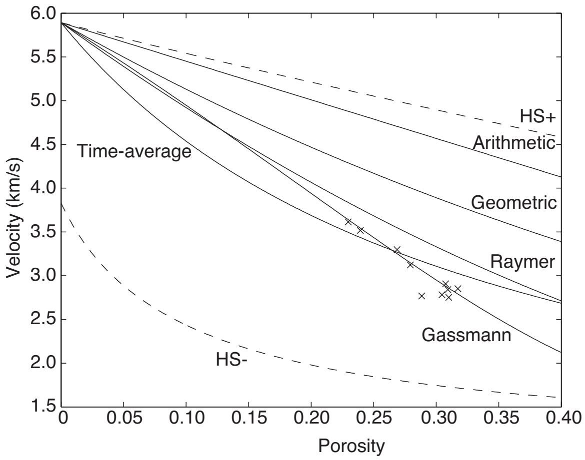

Figure 14. Different models of the P-wave velocity as a function of porosity and real data (crosses), corresponding to the sandy section of the well.

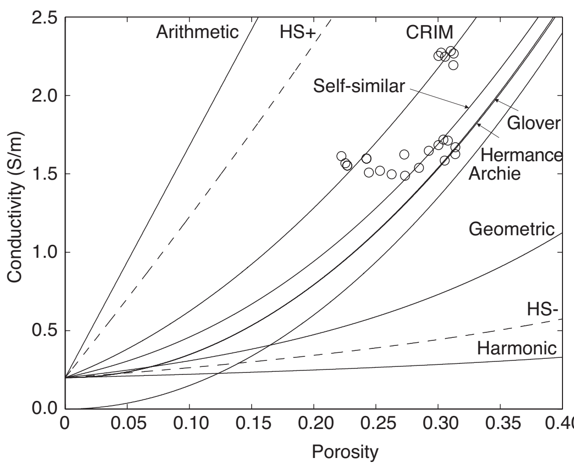

Figure 15. Different models of the conductivity as a function of porosity and real data (circles), corresponding to the shaly section of the well.

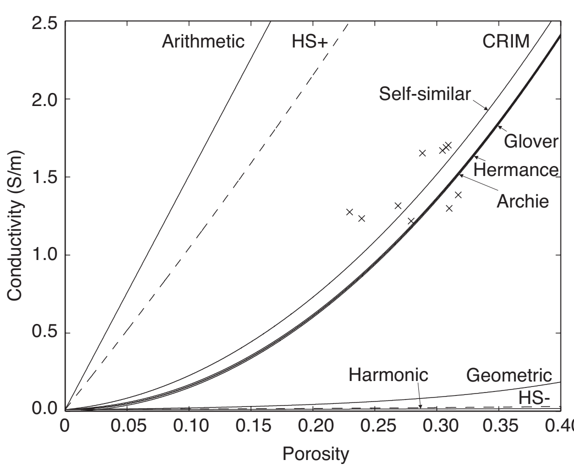

Figure 16. Different models of the conductivity as a function of porosity and real data (crosses), corresponding to the sandy section of the well.

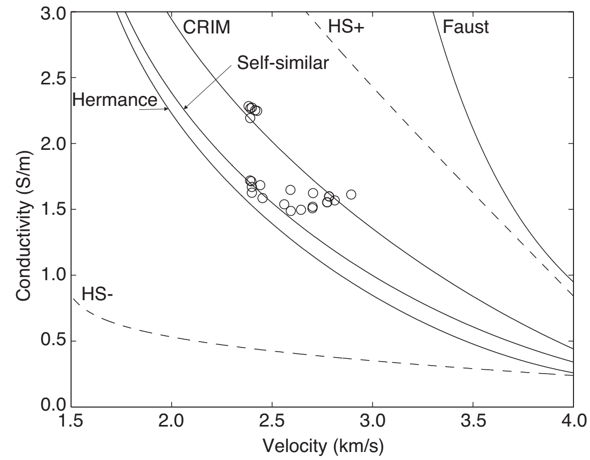

Figure 17. P-wave velocity/conductivity relations based on Gassmann velocity and different models of the electrical conductivity, corresponding to the shaly section of the well.

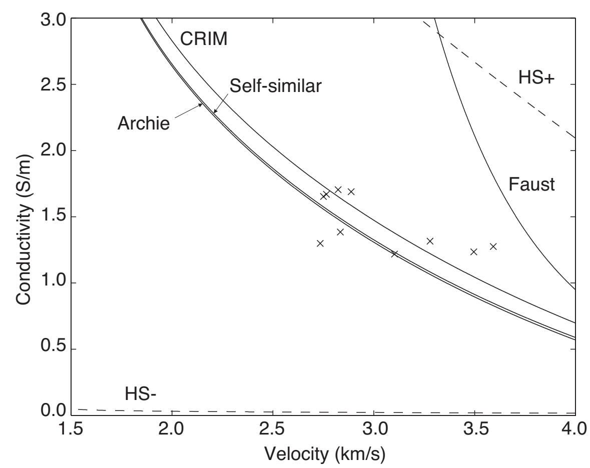

Figure 18. P-wave velocity/conductivity relations based on Gassmann velocity and different models of the electrical conductivity, corresponding to the sandy section of the well.

CONCLUSIONS

Cross-property relations are obtained between the electrical conductivity and seismic velocity using different combinations of the electromagnetic and elastic models. If the HS bounds represent realistic bounds, then, the CRIM and self-similar electrical models are the best choice to obtain reliable cross-property relations. The elastic models are within the bounds generally. The dry-rock modulus based on the Krief model is shown to be within the bounds of well-established theories, such as the Gibiansky-Torquato theory. The Krief model is used to obtain Gassmann (wet-rock) modulus and calculate the seismic velocity. Gassmann-based relations give tight curves for the overburden, while the curves are more dissimilar for the reservoir. The trend is that as the velocity in the overburden (shale saturated with high-conductivity brine) increases, the conductivity decreases. The opposite behavior is obtained for the sandstone (saturated with high-resistivity oil).

The relations have been tested with well-log data of the North Sea. Several of them, in particular the Gassmann/CRIM and Gassmann/

self-similar relations, provide a reasonable fit to the data, indicating that it is possible to predict an electrical property from an elastic property, and vice versa. However, there is a need to identify each relation with a specific type of sediment or rock. In this sense, the different relations must be tested with controlled real data, such as laboratory experiments on synthetic and real rocks. To our knowledge, there seems to be a complete lack of these types of data for rocks. The next stage of the research is to perform such tests and determine the more reliable cross-property relations.

ACKNOWLEDGMENTS

We acknowledge financial support from EMGS, Norsk Hydro, Statoil, and the Norwegian Research Council via the PRIME project at NTNU.

REFERENCES

Archie, G. E., 1942, The electrical resistivity log as an aid in determining some reservoir characteristics: Petroleum Technology, **1**, 55–67.

Berryman, J. G., 1995, Mixture theories for rock properties *in* T. J. Ahrens, ed., Rock physics and phase relations. A handbook of physical constants: American Geophysical Union Reference Shelf 3, 205–228.

Berryman, J. G., and G. W. Milton, 1988, Microgeometry of random composites and porous media: Journal of Physics D, **21**, 87–94.

Bristow, J. R., 1960, Microcracks, and the static and dynamic elastic constants of annealed heavily coldworked metals: British Journal of Applied Physics, **11**, 81–85.

Brito Dos Santos, W. L., T. J. Ulrych, and O. A. L. De Lima, 1988, A new approach for deriving pseudovelocity logs from resistivity logs: Geophysical Prospecting, **36**, 83–91.

Bussian, A. E., 1983, Electrical conductance in a porous medium: Geophysics, **48**, 1258–1268.

Carcione, J. M., 2007, Wave fields in real media. Theory and numerical simulation of wave propagation in anisotropic, anelastic, porous and electromagnetic media, 2nd ed.: Elsevier Science Publ. Co., Inc.

Carcione, J. M., M. Landrø, A. F. Gangi, and F. Cavallini, 2006a, Determining the dilation factor in 4D monitoring of compacting reservoirs by rock-physics models: Geophysical Prospecting, http://dx.doi.org/10.1111/j.1365-2478.2007.00633.x.

Carcione, J. M., S. Picotti, D. Gei, and G. Rossi, 2006b, Physics and seismic modeling for monitoring CO_2 storage: Pure and Applied Geophysics, **163**, 175–207.

Carcione, J. M., and G. Seriani, 2000, An electromagnetic modelling tool for the detection of hydrocarbons in the subsoil: Geophysical Prospecting, **48**, 231–256.

Carcione, J. M., G. Seriani, and D. Gei, 2003, Acoustic and electromagnetic properties of soils saturated with salt water and NAPL: Journal of Applied Geophysics, **52**, 177–191.

De Witte, A. J., 1957, Saturation and porosity from electric logs in shaly sands: Oil and Gas Journal, **55**(9), 89–97.

Faust, L. Y., 1953, A velocity function including lithologic variation: Geophysics, **18**, 271–288.

Gibiansky, L. V., and S. Torquato, 1995, Connection between the conductivity and bulk modulus of isotropic composite materials: Philosophical Transactions of the Royal Society of London, **A353**, 243–278.

———, 1996a, Rigorous link between the conductivity and elastic moduli of fiber reinforced materials: Proceedings of the Royal Society, A452, 253–283.

———, 1996b, Bounds on the effective moduli of cracked materials: Journal of the Mechanics and Physics of Solids, **44**, 233–242.

Glover, P. W. J., M. J. Hole, and J. Pous, 2000, A modified Archie's law for two conducting phases: Earth and Planetary Science Letters, **180**, 369–383.

Glover, P. W. J., I. I. Zadjali, and K. A. Frew, 2006, Permeability prediction from MICP and NMR data using and electrokinetic approach: Geophysics, **71**, no. 4, F49–F60.

Hacikoylu, P., J. Dvorkin, and G. Mavko, 2006, Resistivity-velocity transforms revisited: The Leading Edge, **25**, 1006–1009.

Hermance, J. F., 1979, The electrical conductivity of materials containing partial melt, a simple model from Archie's law: Geophysical Research Letters, **6**, 613–616.

Ikwuakor, K. C., 2007, Comments on "Resistivity-velocity transforms revisited": The Leading Edge, **26**, 134–137.

Kachanov, M., I. Sevostianov, and B. Shafiro, 2001, Explicit cross-property correlations for porous materials with anisotropic microstructures: Journal of the Mechanics and Physics of Solids, **49**, 1–25.

Kennedy, W. D., and D. C. Herrick, 2004, Conductivity anisotropy in shale-free sandstone: Petrophysics, **45**, 30–58.

Krief, M., J. Garat, J. Stellingwerff, and J. Ventre, 1990, A petrophysical interpretation using the velocities of P and S waves (full waveform sonic): The Log Analyst, **31**, 355–369.

Markov, K. Z., 1999, Elementary micromechanics of heterogeneous media, *in* K. Z. Markov and L. Preziosi, eds., Heterogeneous Media: Micromechanics modeling methods and simulations: Birkhauser-Verlag, 1–162.

Mavko, K. Z., T. Mukerji, and J. Dvorkin, 1998, The rock physics handbook: Tools for seismic analysis in porous media: Cambridge University Press.

Milton, G. W., 1981, Bounds on the electromagnetic, elastic and other properties of two-component composites: Physical Review Letters, **46**, 542–545.

———, 1997, Composites: A myriad of microstructure independent relations, T. Tatsumi, E. Watanabe, and T. Kambe, eds., Theoretical and applied mechanics, Proceedings of the XIX International Congress of Theoretical and Applied Mechanics: Elsevier Science Publ. Co., Inc., 443–459.

Mindlin, R. D., 1949, Compliance of elastic bodies in contact: Journal of Applied Mechanics, **16**, 259–268.

Postma, G. W., 1955, Wave propagation in a stratified medium: Geophysics, **20**, 780–806.

Pride, S., 1994, Governing equations for the coupled electromagnetics and acoustic of porous media: Physical Review B, **50**, 15678–15696.

Raymer, L. L., E. R. Hunt, and J. S. Gardner, 1980, An improved sonic transit time to porosity transform: 21st Annual Logging Symposium, Transactions of the Society of Professional Well Log Analysts, Paper 546.

Schön, J. H., 1996, Physical properties of rocks: Fundamentals and principles of petrophysics, Pergamon Press, Inc.

Sen, P. N., C. Scala, and M. H. Cohen, 1981, A self-similar model for sedimentary rocks with applications to the dielectric constant of fused glass beads: Geophysics, **46**, 781–795.

Sevostianov, I., and M. Kachanov, 2007, Connections between elastic and conductive properties of heterogeneous materials: http://me.nmsu.edu/~igor/Sevastianov-Kachanov-text.doc.

White, J. E., N. G. Mikhaylova, and F. M. Lyakhovitskiy, 1975, Low-frequency seismic waves in fluid saturated layered rocks: Izvestija Academy of Sciences USSR, Physics of the Solid Earth, **11**, 654–659.